SFQ/DQFP Interface Circuits

Tahereh Jabbari and Eby G. Friedman

Department of Electrical and Computer Engineering University of Rochester, Rochester, New York 14627 tjabbari,friedman@ece.rochester.edu

Abstract—The increasing complexity of hybrid superconductive computing systems has made interface circuits between logic families an issue of growing importance. In this paper, interface circuits between single flux quantum (SFQ) and directly coupled quantum flux parametron (DQFP) logic families to achieve high speed, low power hybrid superconductive computing systems are presented. In the proposed DQFP-to-SFQ interface, margins greater than ±20% for the critical current of the JJs, bias currents, and inductances are exhibited. The margins of the excitation current of the DQFP buffer are -38% and +35% with the frequency of the excitation current in the range of 2 GHz to 10 GHz. In the proposed SFQ-to-DQFP interface, the margins are greater than -33% and +25%. The margins of the excitation current of the DQFP buffer are -50% and +20% for frequencies ranging from 2 GHz to 10 GHz. Since no transformers are required, the physical area of the adiabatic portion of the interface circuits is significantly less than existing interface circuits. The SFQ-to-DQFP interface circuit operates at frequencies approaching 20 GHz. These interface circuits therefore exhibit high parameter margins and operating frequencies while requiring significantly less area as compared to existing interface circuits. The proposed interface circuits support the use of both ultra-low power and high speed logic families in complex hybrid superconductive systems.

Index Terms—Single flux quantum, adiabatic quantum flux parametron, directly coupled quantum flux parametron, superconductive integrated circuits.

I. INTRODUCTION

uperconductive electronics is a highly promising, albeit superconductive electronics is a nightly promising, albeit cryogenic, beyond CMOS technology for prospective exascale computing systems, which enable ultra-low power and ultra-high speed integrated circuits [1]-[5]. Superconductive single flux quantum (SFQ) technology exhibits switching delays on the order of a few picoseconds and switching energies of approximately 10 ⁻¹⁹ Joules [2], [6], [7]. Superconductive SFQ technology has been demonstrated to operate at frequencies approaching 80 GHz for an RSFQ arithmetic logic unit with an 8 bit datapath [8]. Adiabatic superconductive circuits, such as adiabatic quantum flux parametron (AQFP) [9]-[15] and directly coupled quantum flux parametron (DQFP) [16]-[18], are highly energy efficient logic families. The dynamic power consumption of AQFP circuits is reduced by adiabatic operation to a switching energy of $0.03 \times I_c \Phi_0$, where I_c and Φ_0 are, respectively, the critical current of a Josephson junction

The effort depicted is supported by the National Science Foundation under Grant No. 2124453 and the Department of Defense Agency Intelligence Advanced Research Projects Activity through the U.S. Army Research Office under Contract No. W911NF-17-9-0001. The content of the information does not necessarily reflect the position or the policy of the Government, and no official endorsement should be inferred.

(JJ) and a single flux quantum. AQFP circuits dissipate two to three orders of magnitude lower power than SFQ circuits. AQFP circuits however typically operate at much lower frequencies than SFQ circuits.

A hybrid computing system, composed of both SFQ and AQFP logic families, provides both ultra-high speed and extremely low power operation. Interface circuits are therefore required to transfer data between the SFQ and AQFP circuitry. A standard AQFP-to-SFQ interface includes eleven Josephson junctions (JJs) and two transformers, requiring significant bias current and physical area [19], [20]. These standard AQFP/SFQ interface circuits also exhibit narrow parameter margins and operate at low frequencies. To achieve high speed, hybrid computing systems, enhanced AQFP/SFQ interface circuits are desirable to transfer data between the AQFP and SFQ circuitry. These circuits should require low area, exhibit effective parameter margins, and operate at high frequencies.

In this paper, interface circuits between adiabatic logic circuits and SFQ logic circuits are proposed. Directly coupled quantum flux parametron logic is reviewed in section II. A novel DQFP-to-SFQ interface requiring less area and improved parameter margins is described in section III. A novel SFQ-to-DQFP interface is proposed in section IV. The effects of the circuit parameters on the performance of the DQFP-to-SFQ and SFQ-to-DQFP interfaces are also described, respectively, in sections III and IV. The paper is concluded in section V.

II. DQFP LOGIC

Directly coupled quantum flux parametron (DQFP) logic is power and area efficient. DQFP logic operates adiabatically, similar to AQFP logic [9], [16], [17], [21]. Due to adiabatic switching, DQFP dissipates bit energy per switching similar to AQFP [17]. An AQFP buffer gate is shown in Fig. 1(a). Standard AQFP logic uses signal transformers to propagate and invert the output current, requiring significant area [9]–[11], [21]. A DQFP buffer gate is shown in Fig. 1(b). Unlike AQFP, however, DQFP logic inverts and transfers the output current without requiring signal transformers, thereby requiring significantly less area [16]–[18].

The DQFP buffer is composed of two RF superconductive quantum interference device (SQUID) loops with a shared inductance L_q [9], as shown in Fig. 1(b). Characterization of the JJs within the DQFP buffer is based on the 10 kA/cm² MIT Lincoln Laboratory SFQ5ee fabrication process [22]. The JJs are not damped with resistors to achieve extremely low

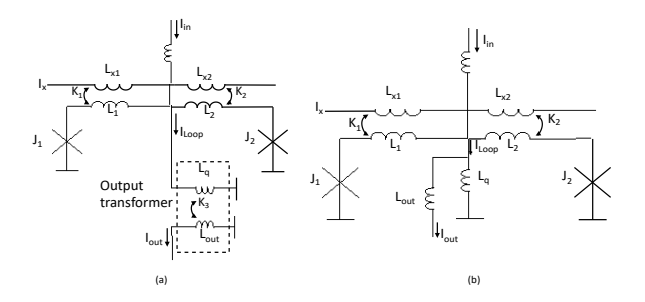


Fig. 1. Buffer logic circuit, (a) AQFP, and (b) DQFP. $L_{x1,2} = 2.1$ pH, $L_{1,2} = 1.3$ pH, $K_{1,2} = 0.35$, J1 = J2 = 200 μ A, $L_q = 10.2$ pH, $K_3 = 0.6$, $L_{out_{AQFP}} = 10$ pH, and $L_{out_{QGPP}} = 1.5$ pH.

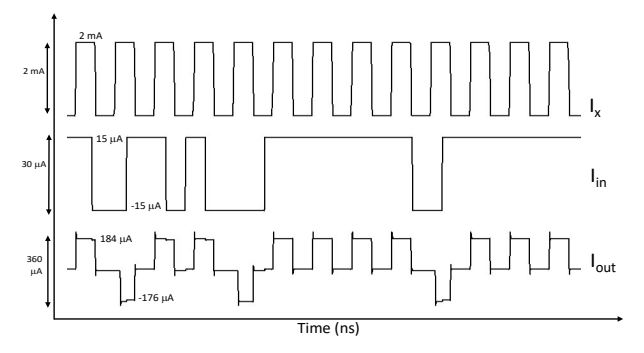


Fig. 2. Operation of DQFP buffer with large JJs. I_x , I_{in} , and I_{out} are, respectively, the AC excitation current, input current, and DC output current. The output current I_{out} of the DQFP buffer is 280μ A.

energy consumption [14]. When the AC excitation current I_x increases, either J1 or J2 switches, producing current through L_q and L_{out} depending upon the direction of the input current I_{in} . A current I_{Loop} is produced within the loop, setting the state of the buffer. The DQFP buffer is area efficient. Unlike an AQFP buffer, I_{out} can be directly transferred to the next stage without a transformer. The state of the buffer is set by the direction of the loop current I_{Loop} , as with AQFP logic.

The output of the DQFP buffer is shown in Fig. 2. The frequency of the excitation current is 2.5 GHz. The output pulse I_{out} is a DC current directly connected to the next stage of either a DQFP or AQFP circuit. The magnitude of the output current is dependent upon the output inductor L_{out} , JJs, and inductor L_{q} within the SQUID loops. The JJs within the DQFP buffer are typically large to produce a high DC output current within the AQFP/DQFP-to-SFQ interface. The operation of the DQFP buffer with these large JJs ($I_{c} = 200~\mu$ A) is shown in Fig. 2 when connected to the DQFP buffer at the input and output ports. The output current I_{out} of the DQFP buffer is $\mathbb{P}180~\mu$ A.

III. DQFP-TO-SFQ INTERFACE

An AQFP-to-SFQ interface circuit [19], [20] transfers data from an adiabatic circuit to an SFQ circuit in a hybrid superconductive digital system. Standard interfaces [19], [20], [23] exhibit small parameter margins, particularly for the JJs within the SFQ portion of the interface, while requiring significant area for the transformer within the AQFP buffer. In the proposed DQFP-to-SFQ interface, the AQFP buffer is replaced with a DQFP buffer. The DQFP buffer transfers

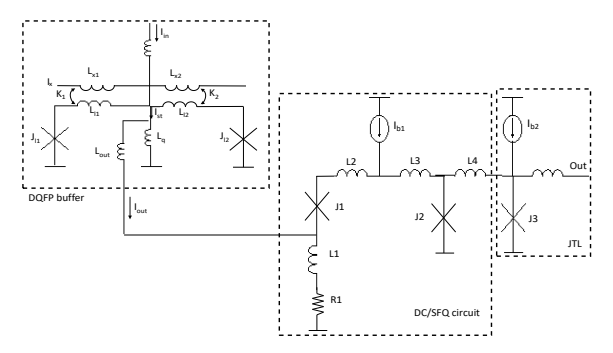


Fig. 3. Proposed DQFP-to-SFQ interface. $L_{x1,2}=2.1$ pH, $L_{1,2}=1.3$ pH, $K_{1,2}=0.35$, J1=J2=200 μ A, $L_{q}=10.4$ pH, $L_{out}_{DQ,F}=1.5$ pH, J1=158 μ A, J2=80 μ A, J3=250 μ A, L1=5.7 pH, L2=0.5 pH, L3=1 pH, L4=10 pH, L5=2 pH, $R_{1}=1$ mQ $I_{b1}=115$ μ A, and $I_{b2}=220$ μ A.

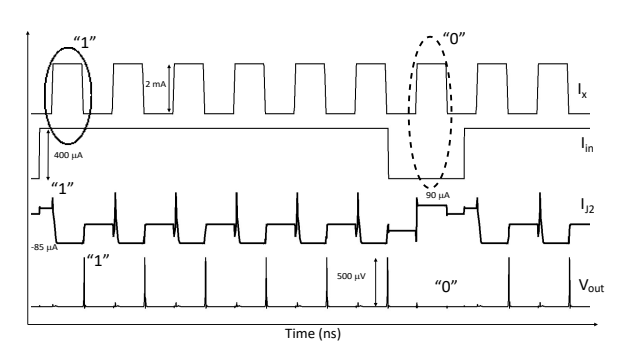


Fig. 4. Waveform characteristics of DQFP-to-SFQ interface. I_x and I_{in} are, respectively, the AC excitation current and input current of the DQFP buffer. $I_{J\,2}$ is the DC current through junction J_2 . In logic state "1" of the DQFP buffer, junction J_2 switches, producing an SFQ pulse. V_{out} is the SFQ output pulse of the DQFP-to-SFQ interface.

output current without requiring transformers, reducing the area of the adiabatic portion of the circuit. The interface also exhibits wider parameter margins.

The proposed DQFP-to-SFQ interface is shown in Fig. 3. The interface is composed of a DQFP buffer and a DC-to-SFQ interface. Three JJs are used in the SFQ portion of the DQFP-to SFQ interface, requiring no signal transformers between the DQFP buffer and the SFQ portion. The output of the DQFP buffer is a DC current. To produce an SFQ pulse, a DC-to-SFQ converter is directly connected to the output of the DQFP buffer. The output of the DQFP-to-SFQ interface is shown in Fig. 4. The frequency of the excitation current is 2.5 GHz. In state "1," where the current at the input of the DC-to-SFQ circuit increases, the DC current through junction $\rm J_2$ exceeds the critical current, switching the junction. Junction $\rm J_3$ operates as a single stage Josephson transmission line (JTL) [7] at the output of the DQFP-to-SFQ interface.

The magnitude of the output current of the DQFP buffer I_{out} affects the performance of the interface. A standard DC-to-SFQ interface operates with a large DC input current [24], [25]. The output DC current of the DQFP and AQFP buffer is dependent upon the size of the JJs. Large JJs with a critical current of 200 μ A are used within standard AQFP-to-SFQ interfaces [20]. For the DQFP buffer to provide greater DC output current, larger JJs are also used within the DQFP buffer (see Section II). The DC-to-SFQ interface within the proposed

DQFP-to-SFQ interface targets an input current ranging from $60~\mu A$ to $160~\mu A$.

For small inductance L_4 , the input DC current is divided between junctions J_2 and J_3 , reducing the negative margin of the input DC current. A large inductance L_4 passes the input DC current through junction J_2 while increasing the overall delay of the DC-to-SFQ converter. The output delay of the SFQ part is 8.5 ps. A tradeoff therefore exists between the negative margin of the input DC current and the signal delay.

The DQFP-to-SFQ interface achieves wider margins as compared to a standard AQFP-to-SFQ interface. The standard AQFP-to-SFQ interface exhibits less than ±10% parameter margins for those JJs in the SFQ portion of the circuit [20], [23]. The distribution of bias currents in the SFQ portion and the offset current within the DQFP buffer significantly suppress the parameter margins. The effects of these currents on the margins within the proposed DQFP-to-SFQ interface can be improved to at least $\pm 20\%$ by adjusting L₁, L₂, L₃, and L₄. The margins of the excitation current of the DQFP buffer are -38% and +35% with the frequency of the excitation current in the range of 2 GHz to 10 GHz. The margins of J_1 and J_2 are, respectively, $\pm 20\%$ and (-40% and +62%). The margins of the bias current I_{b1} are -35% and +20%. The margins of the input inductor L_1 are -26% and +40%. The margins of inductors L₂ to L₄ are -90%, +100%.

IV. SFQ-TO-DQFP INTERFACE CIRCUIT

An SFQ-to-DQFP interface transfers data from an SFQ circuit to an adiabatic circuit. A standard SFQ-to-AQFP interface [19] is composed of two parts, an SFQ part and an AQFP part. These two parts are connected by a transformer [19] which requires significant area. The standard interface also exhibits narrow margins for the JJs within the SFQ part and a low operating frequency [19], [23]. An SFQ-to-DQFP interface with wider parameter margins and higher operating frequencies is proposed here. In this interface, the AQFP buffer is replaced with a DQFP buffer, and no transformers are necessary.

The proposed SFQ-to-DQFP interface is composed of an SFQ-to-DC converter [24] and DQFP buffer, as shown in Fig. 5. The SFQ-to-DC converter is at the input of the interface and produces a DC output voltage. The output characteristics of the SFQ-to-DC converter is composed of a series of SFQ pulses. The output of the SFQ-to-DC converter is directly connected to the DQFP buffer (see Fig. 5).

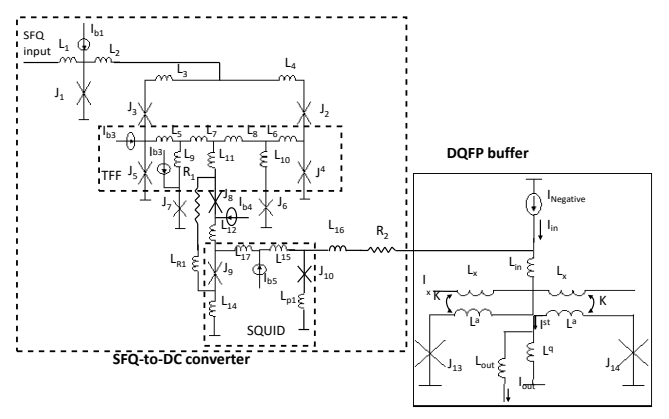


Fig. 5. Proposed SFQ-to-DQFP interface. L $_{X}$ = 2.1 pH, L $_{a}$ = 1.46 pH, K $_{1,2}$ = 0.35, J1 = J2 = 200 μ A, L $_{q}$ = 12.4 pH, L $_{out}$ D Q F P = 2 pH, L $_{in}$ D Q F P = 15.3 pH, R2 = 1.5 ω , and I N egative = -20 μ A.

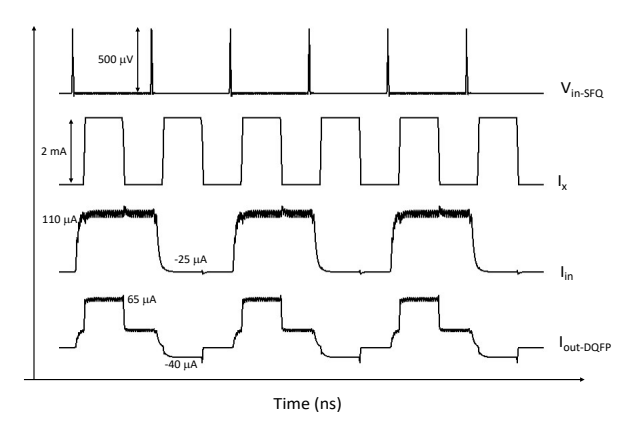


Fig. 6. Operation of SFQ-to-DQFP interface. V_{in-SFQ} is the input of the SFQ-to-DQFP interface. I_x and $I_{in-DQFP}$ are, respectively, the AC excitation current and input current of the DQFP buffer. $I_{Out-DQFP}$ is the DC output current of the SFQ-to-DQFP interface.

The SFQ-to-DC interface includes a T flip flop (TFF) at the input and a SQUID loop at the output (see Fig. 5). The incoming pulse stores a flux quantum inside the TFF. Due to the stored flux quantum and current within the TFF, the JJs within the SQUID, J_9 and J_{10} , are biased above the critical current to produce a series of SFQ voltage pulses. The average of these pulses is a DC voltage. The next incoming SFQ pulse releases the stored flux within the TFF. The JJs within the SQUID are biased below the critical current. The circuit produces zero voltage (the absence of an SFQ pulse) at the output.

To produce both logic states within the DQFP buffer of the SFQ-to-DQFP interface, a bidirectional DC current at the input of the DQFP buffer is required. The SFQ portion of the SFQ-to-DQFP interface, the SFQ-to-DC converter, provides a positive DC current to produce logical state "1" within the DQFP buffer. An additional negative DC current I_{Negative} is added at the input of the DQFP buffer to produce logical state "0" within the DQFP buffer. Both states of the DQFP buffer are synchronized by the excitation current I_{x} .

The output of the SFQ-to-DQFP interface is shown in Fig. 6. The frequency of the excitation current is 2.5 GHz. To provide a small DC current at the output of the DQFP buffer, small

JJs with a critical current of 50 μA are used within the DQFP buffer. With these small JJs, the peak-to-peak magnitude of the output current I_{Out-DQFP} of the SFQ-to-DQFP interface is approximately 100 μA .

The SFQ-to-DC converter within the interface produces an offset current as well as fluctuations within the inductive loops of the DQFP buffer. These fluctuations occur due to the series of SFQ pulses at the output of the SFQ-to-DC converter. To manage the offset current and fluctuations, a resistor is placed in series with the output inductance of the SFQ-to-DC circuit.

The effects of the resistor on the performance of the SFQto-DQFP interface are shown in Figs. 7(a) and 7(b). The slow decay time - the time to achieve sufficient negative current - of the current due to the small resistor (see Fig. 7(a)) produces incorrect operation within the SFQ-to-DQFP interface when operating at high frequencies while decreasing the signal fluctuations in the input signal of the DQFP buffer. A large resistor decays the signal more quickly while increasing the fluctuations at the input of the DQFP buffer (see Fig. 7(b)). A tradeoff therefore exists between the decay time and the signal fluctuations. The operating frequency of the SFQ-to-DQFP interface is also impacted by the resistor. A large resistor produces a shorter decay time while increasing fluctuations in the signal (see Fig. 7(b)). Due to the short decay time, the SFQ-to-DQFP interface with a large resistor can operate at a higher frequency, up to 20 GHz.

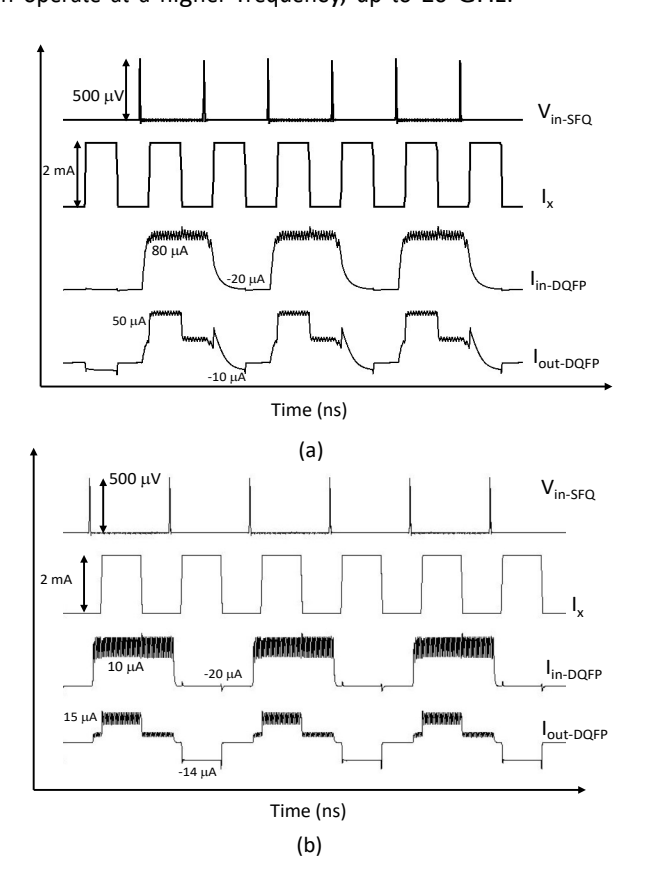


Fig. 7. Effects of the resistor within the SFQ-to-DQFP interface, (a) small resistor, and (b) large resistor. $V_{i\,n\,-S\,F\,Q}$ is the input of the SFQ-to-DQFP interface. I_x and $I_{i\,n\,-D\,Q\,F\,P}$ are, respectively, the AC excitation current and input current of the DQFP buffer. I_{out} is the DC output current of the SFQ-to-DQFP interface. The small resistor lowers the signal fluctuations while increasing the decay time.

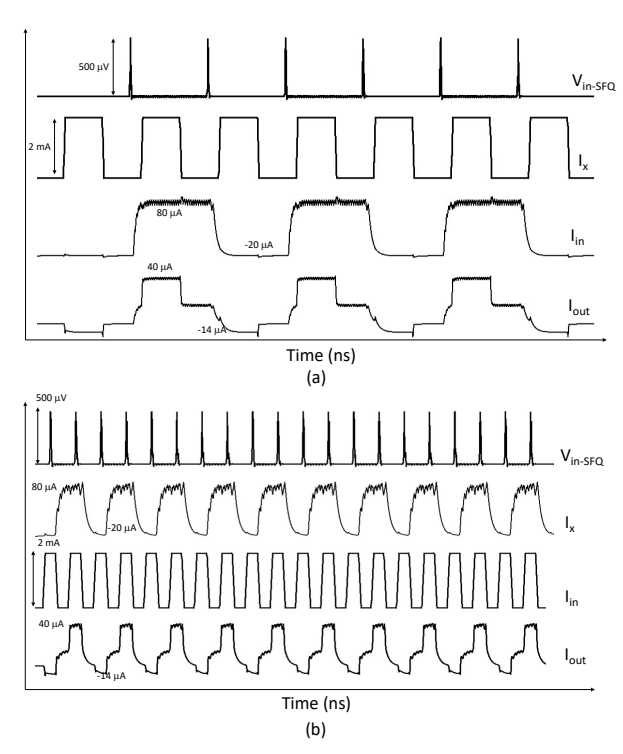


Fig. 8. Operation of the proposed SFQ-to-DQFP interface, (a) 2 GHz, and (b) 10 GHz. V $_{i\,n-S\,F\,Q}$ is the input SFQ pulse of the SFQ-to-DQFP interface. Ix and I $_{i\,n}$ are, respectively, the AC excitation current and input current of the DQFP buffer. Iout is the DC output current of the SFQ-to-DQFP interface.

The resistor at the input of the DQFP buffer significantly affects the parameter margins. A small resistor improves the margins of all of the parameters. A 1 Ω resistor effectively removes any offset currents and fluctuations within the DQFP buffer while not significantly degrading the operation of the interface. The waveform characteristics of the proposed SFQto-DQFP interface at 2 GHz and 10 GHz are, respectively, illustrated in Figs. 8(a) and 8(b). In the proposed SFQ-to-DQFP interface, the margins of all parameters including the bias currents, inductors, and JJs are greater than -33% and +25%. The margins of the excitation current of the DQFP buffer are -50% and +20% from 2 GHz to 10 GHz. Future research to enhance the interface and verify the advantages in terms of the area, margins, and operating frequency include parameter optimization, physical design, and post-layout parameter extraction.

V. CONCLUSIONS

Superconductive digital circuits utilizing different logic families require an interface. Interfaces between superconductive adiabatic logic and SFQ logic are presented in this paper. The interfaces exhibit small area, wide margins, and high operating frequencies as compared to standard SFQ/AQFP interfaces. A DQFP buffer is used rather than an AQFP buffer, significantly reducing area. In the DQFP-to-SFQ interface, the parameter margins are greater than ±20%. The margins in the SFQ-to-DQFP interface are greater than -33% and +25%. The SFQ-to-DQFP interface operates at frequencies approaching 20 GHz. Tradeoffs for the proposed interfaces among the delay, parameter margins, decay time, and signal fluctuations are also discussed.

REFERENCES

- G. Krylov and E. G. Friedman, Single Flux Quantum Integrated Circuit Design. Springer Publishers, 2022.
- [2] T. Jabbari and E. G. Friedman, "Global Interconnects in VLSI Complexity Single Flux Quantum Systems," Proceedings of the Workshop on System-Level Interconnect: Problems and Pathfinding Workshop, pp. 1–7, November 2020.
- [3] T. Jabbari and E. G. Friedman, "Surface Inductance of Superconductive Striplines," IEEE Transactions on Circuits and Systems II: Express Briefs, vol. 69, no. 6, pp. 2952–2956, June 2022.
- [4] R. Bairamkulov, T. Jabbari, and E. G. Friedman, "QuCTS-Single Flux Quantum Clock Tree Synthesis," IEEE Transactions on Computer-Aided Design of Integrated Circuits and Systems, vol. 41, no. 10, pp. 3346 – 3358. October 2022.
- [5] T. Jabbari and E. G. Friedman, "Flux Mitigation in Wide Superconductive Striplines," IEEE Transactions on Applied Superconductivity, vol. 32, no. 3, pp. 1–6, February 2022.
- [6] T. Jabbari, G. Krylov, S. Whiteley, J. Kawa, and E. G. Friedman, "Repeater Insertion in SFQ Interconnect," IEEE Transactions on Applied Superconductivity, vol. 30, no. 8, p. 5400508, December 2020.
- [7] T. Jabbari, G. Krylov, S. Whiteley, E. Mlinar, J. Kawa, and E. G. Friedman, "Interconnect Routing for Large Scale RSFQ Circuits," IEEE Transactions on Applied Superconductivity, vol. 29, no. 5, August 2019.
- [8] J. Y. Kim and J. H. Kang, "High Frequency Operation of a Rapid Single Flux Quantum Arithmetic and Logic Unit," Journal of the Korean Physical Society, vol. 48, no. 5, pp. 1004–1007, May 2006.
- [9] N. Takeuchi, Y. Yamanashi, and N. Yoshikawa, "Adiabatic Quantum-Flux-Parametron Cell Library Adopting Minimalist Design," Journal of Applied Physics, vol. 117, no. 17, p. 173912, May 2015.
- [10] N. Takeuchi, D. Ozawa, Y. Yamanashi, and N. Yoshikawa, "An Adiabatic Quantum Flux Parametron as an Ultra-Low-Power Logic Device," Superconductor Science and Technology, vol. 26, no. 3, p. 035010, January 2013.
- [11] N. Takeuchi, Y. Yamanashi, and N. Yoshikawa, "Energy Efficiency of Adiabatic Superconductor Logic," Superconductor Science and Technology, vol. 28, no. 1, p. 015003, November 2014.
- [12] C. J. Fourie, N. Takeuchi, K. Jackman, and N. Yoshikawa, "Evaluation of Flux Trapping Moat Position on AQFP Cell Performance," Journal of Physics: Conference Series, vol. 1975, no. 012027, pp. 1–6, December 2020.
- [13] N. Takeuchi, H. Suzuki, C. J. Fourie, and N. Yoshikawa, "Impedance Design of Excitation Lines in Adiabatic Quantum-Flux-Parametron Logic Using InductEx," IEEE Transactions on Applied Superconductivity, vol. 31, no. 5, p. 1300605, August 2021.
- [14] Y. He, C. L. Ayala, N. Takeuchi, T. Yamae, Y. Hironaka, A. Sahu, V. Gupta, A. Talalaevskii, D. Gupta, and N. Yoshikawa, "A Compact AQFP Logic Cell Design Using an 8-Metal Layer Superconductor Process," Superconductor Science and Technology, vol. 33, no. 3, p. 035010, February 2020.
- [15] Y. Hironaka, S. S. Meher, C. L. Ayala, Y. He, T. Tanaka, M. Habib, A. Sahu, A. Inamdar, D. Gupta, and N. Yoshikawa, "Demonstration of Interface Circuits for Adiabatic Quantum-Flux-Parametron Cell Library Using an Eight-Metal Layer Superconductor Process," IEEE Transactions on Applied Superconductivity, vol. 33, no. 5, pp. 1–5, August 2023.
- [16] R. Ishida, N. Takeuchi, T. Yamae, and N. Yoshikawa, "Parameter Optimization of Directly Coupled Quantum Flux Parametron Circuits," IEICE Technical Report, vol. 119, no. 369, pp. 91–93, January 2020.
- [17] N. Takeuchi, K. Arai, and N. Yoshikawa, "Directly Coupled Adiabatic Superconductor Logic," Superconductor Science and Technology, vol. 33, no. 6, p. 065002, May 2020.
- [18] R. Ishida, N. Takeuchi, T. Yamae, and N. Yoshikawa, "Design and Demonstration of Directly Coupled Quantum-Flux-Parametron Circuits With Optimized Parameters," IEEE Transactions on Applied Superconductivity, vol. 31, no. 5, p. 1100505, August 2021.
- [19] F. China, N. Tsuji, T. Narama, N. Takeuchi, T. Ortlepp, Y. Yamanashi, and N. Yoshikawa, "Demonstration of Signal Transmission Between Adiabatic Quantum-Flux-Parametrons and Rapid Single-Flux-Quantum Circuits Using Superconductive Microstrip Lines," IEEE Transactions on Applied Superconductivity, vol. 27, no. 4, pp. 1–5, June 2017.
- [20] F. China, T. Narama, N. Takeuchi, T. Ortlepp, Y. Yamanashi, and N. Yoshikawa, "Design and Demonstration of Interface Circuits Between Rapid Single-Flux-Quantum and Adiabatic Quantum-Flux-Parametron Circuits," IEEE Transactions on Applied Superconductivity, vol. 26, no. 5, p. 1301305, August 2016.

- [21] N. Takeuchi, T. Yamae, C. L. Ayala, H. Suzuki, and N. Yoshikawa, "An Adiabatic Superconductor 8-bit Adder with 24kBT Energy Dissipation per Junction," Applied Physics Letters, vol. 114, no. 4, p. 042602, January 2019.
- [22] S. K. Tolpygo, V. Bolkhovsky, T. J. Weir, A. Wynn, D. E. Oates, L. M. Johnson, and M. A. Gouker, "Advanced Fabrication Processes for Superconducting Very Large-Scale Integrated Circuits," IEEE Transactions on Applied Superconductivity, vol. 26, no. 3, pp. 1–10, April 2016.
- [23] Y. He, C. L. Ayala, N. Takeuchi, Y. Hironaka, T. Yamae, S. Meher, A. Inamdar, D. Gupta, and N. Yoshikawa, "Demonstration of Interfaces Between Adiabatic Quantum-Flux-Parametron and Rapid Single-Flux-Quantum Circuits Using the MIT-LL SFQ5ee Process," Applied Superconductivity Conference, November 2020.
- [24] "RSFQ Cell Library." [Online]. Available: https://wwwalt.tuilmenau.de/it-tet/forschung/supraleitende-hochgeschwindigkeitselektronik/rsfq-cell/interfaces/
- [25] K. K. Likharev and V. K. Semenov, "RSFQ Logic/Memory Fam-ily: A New Josephson-Junction Technology for Sub-Terahertz-Clock-Frequency Digital Systems," IEEE Transactions on Applied Superconductivity, vol. 1, no. 1, pp. 3–28, March 1991.